Using RocFall3 to Investigate the Rockfall Hazard Process on Highly Fractured Rocky Hills, Yaounde, Cameroon

Roger Bissaya[1(✉)], Robert Eko Medjo[1,2], Richard Tanwi Ghogomu[1], Bernard Njom[1], and Bernadin Bohi[2]

[1] Department of Earth Sciences, University of Yaounde 1, Yaounde, Cameroon
rogerbissaya@gmail.com
[2] Ecole Nationale Des Ponts Et Chaussées, Abidjan, Ivory Coast

Abstract. Overs the last few years, several rocky hills have undergone voluminous mass movements in the Yaounde area. A first check analysis of rock and slope properties suggests that rockfalls or collapses are the most likely mode of failure in this area. This paper considers the feasibility of using RocFall3 program to help further clarify this hazard process through a case study. Therefore we set theoretical values for translational velocity (30–50 m/s) and rotational velocity (0 or 10°/s). We had as results, long and short almost rectilinear and curved/deviated paths illustrating the targets of the fallen blocks. The 30 m/s translational velocity matches with short length runout, whereas the 50 m/s translational velocity matches with long length runout. Since the slopes are difficult to achieve in the field, this simulation provided concrete overview of the phenomenon and some basic physical parameters to be retained. However, the work has been based solely on simplified/idealized models that may not be wholly representative of real field conditions.

Keywords: joint · rock paths · rock slope · models · Cameroon

1 Introduction

A rockfall is a rapid mass movement generated by the detachment of a rock volume from a slope that falls, bounces, and rolls during its propagation downhill (Varnes 1978; Hungr et al. 2014). In a rockfall, the initial mobilized mass can be either a single massive block or a set of blocks defined by the joint system in the massif so that the concept of *in situ* block size distribution was introduced by Lu and Latham (1999) and Ruiz-Carulla et al. (2019) to describe the initial distribution of block sizes within the rock mass. This argument is also supported by previous studies (e. g., Merritt and Baecher 1981; Palmström 1995, 2002) and recent studies in the Yaounde area (see Bissaya et al. 2022a, b) which is dominated by high reliefs (Fig. 1). The rocks that make up these high reliefs are highly fracturated by three main joint sets. The block shapes and sizes are supported by the joint network crosscuts. The basement structure is therefore fragile due to the discontinuity weaknesses (Bissaya et al. 2023). Overs the last few years,

R. E. Hammah et al. (Eds.): RIC 2023, AHE 19, pp. 835–846, 2023.
https://doi.org/10.2991/978-94-6463-258-3_78

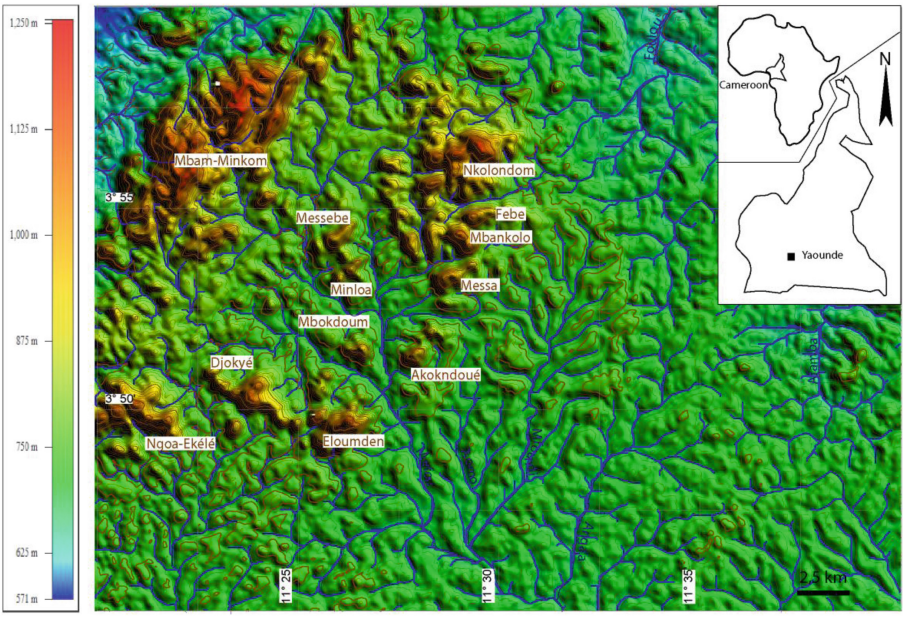

Fig. 1. Location and physiography of the study area showing the high reliefs. The numerical model is derived from the SRTM (Shuttle Radar Topographic Mission) release

several rocky hills (e. g., Mbankolo, Mbokdoum, Akokndoué, Mvog-Betsi, Messebe, etc.) have undergone voluminous mass movements that we consider to be rockfalls (neo and paleo rockfalls). A further check analysis with theoretical values (which are defined by physics laws) within RocFall3 program (where significant improvements have been made in rockfall analysis, particularly in determining rock paths, rock endpoints, and impact locations) is going to help us clarify this statement. To achieve the aforementioned objective, a simplified model of an existing slope will be built and the phenomenon will be analyzed; with reference to seeders and endpoints observed in the field.

2 Slope Stability Framework

2.1 Aspect of the Seeder

In the study area, the seeder is often a sub-vertical plane (or cliff) whose trace could be simplified by a line on the map. In the eastern slope of Mbankolo hill (study case), it is a NW-SE striking cliff which reveals the influence of the jointing patterns of the rock mass. Also, it may show the process of disaggregation of the rock mass by the removal of blocks individual or per rock group.

2.2 Evolvement of the Safety Factor

In this section, we are addressing a quick check to recall how the sensitivity of the safety factor relates to triggering factors.

Given a slope block with a height H = 10 m and inclination $\psi = 85°$, the potential failure plane dips out of rock face at $\Theta = 15°$. The length of the sliding surface is 8 m (L) (see Fig. 2). By limit equilibrium theory, (1) the safety factor of the slope dry (FS), (2) that of the slope saturated, free draining (FSsat'), (2) and that of the slope saturated, ice dammed (FSsat") evolve as we are going to show below.

Additional data: $\gamma_{rock} = 26$ kN/m^3; $\gamma_w = 10$ kN/m^3; $\varphi = 36°$; c = 90 kN/m^2; a = L * 1', where: γ_{rock} is unit weight of rock, γ_w is unit weight of water, φ is friction angle, c is cohesion, a is area of sliding surface for a "unit slope block", 1' is unit slope, A is section of the unit slope block.

It is interesting to note that, in this case there is contact only on sliding plane; cohesion with surrounding blocks is considered set equal to zero. The other planes are considered as release planes.

- t, T, and A:

$$t = \frac{H}{\tan \Psi} = \frac{10\,m}{tan85°} = 0,87\,m$$

$$T = \mathrm{L} - \mathrm{t} = 8 - 0.87 = 7.13\,m$$

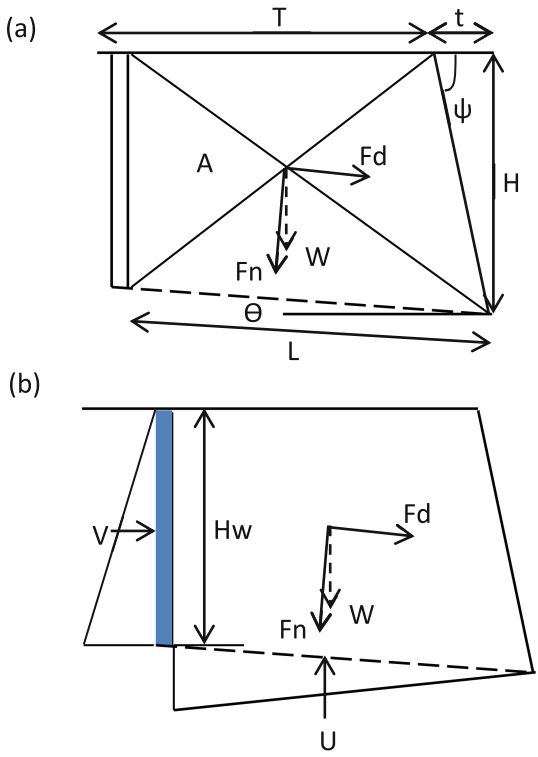

Fig. 2. Slope block section: (a) slope dry and (b) slope saturated

$$A = \frac{(T+L)H}{2} = \frac{(7.13\,m + 8\,m)10\,m}{2} = 75.65\,m^2$$

- Volume of sliding mass (V):

$$V = A * 1^{'} = 75.65m^2 * 1^{'}m = 75.65(1^{'})m^3$$

- Weight (W):

$$W = V * \gamma_{rock} = 75.65\left(1^{'}\right)m^{3} * 26\frac{kN}{m^3} = 1966.9(1^{'})\,kN$$

- Driving force (Fd):

$$Fd = W\sin\theta = 1966.9\left(1'\right)kN * \sin 15^{\circ} = 509.07\left(1'\right)kN$$

- Normal forces (Fn):

$$Fn = W\cos\theta = 1966.9\left(1'\right)kN * \cos 15 = 1899.88\left(1'\right)kN$$

- Resisting force (Fr):

$$Fr = ca + Fn\tan\varphi = 90\frac{kN}{m^2} * 8\left(1^{'}\right)m^2 + 1899.88\left(1^{'}\right)kN\tan 36^{\circ} = 2100.34(1^{'})\,kN$$

- **Safety Factor for dry slope (FS):**

$$FS = \frac{Fr}{Fd} = \frac{2100.34\left(1^{'}\right)kN}{509.07\left(1'\right)kN} = 4.13$$

- Uplift force (U) and thrust force (V), free draining:
  - U free draining:

$$U_1 = \frac{1}{4}a\gamma_w H_w = \frac{8\left(1^{'}\right)m^2 * 10\frac{kN}{m^3} * 10m}{4} = 200\left(1^{'}\right)kN$$

  - V free draining:

$$V_1 = \frac{1}{4}\gamma_w H_w^2 = \frac{10\frac{kN}{m^3} * 100m^2 * \left(1^{'}\right)m}{4} = 250\left(1^{'}\right)kN$$

- **Safety Factor for saturated slope, free draining (FSsat'):**

$$FSsat' = \frac{ca + (Fn - U_1 - V_1\sin\theta)tan\varphi}{Fd + V_1\cos\theta}$$

$$= \frac{90\frac{kN}{m^2} * 8(1')m^2 + \left(1899.88(1')kN - 200(1')kN - 250(1')kN\sin 15^{\circ}\right)\tan 36^{\circ}}{509.07(1')kN + 250(1')kN * \cos 15^{\circ}}$$

$$= 2.54$$

- Uplift force (U) and thrust force (V), ice dammed:
  - U ice dammed:

$$U_2 = \frac{1}{2} a \gamma_w H_w = \frac{8\left(1'\right) m^2 * 10 \frac{kN}{m^3} * 10m}{2} = 400\left(1'\right) kN$$

  - V ice dammed:

$$V_2 = \frac{1}{2} \gamma_w H_w^2 = \frac{10 \frac{kN}{m^3} * 100 m^2 * \left(1'\right) m}{2} = 500\left(1'\right) kN$$

- **Safety Factor for saturated slope, ice dammed (FSsat")**:

$$FSsat' = \frac{ca + (Fn - U_2 - V_2 \sin\theta) tan\varphi}{Fd + V_2 \cos\theta}$$

$$= \frac{90 \frac{kN}{m^2} * 8(1')m^2 + (1899.88(1')kN - 400(1')kN - 500(1')kN * \sin 15°) \tan 36°}{509.07(1')kN + 500(1')kN * \cos 15°}$$

$$= 1.73$$

Assuming that the slope block is theoretically unsafe if FS $\leq$ 1.0 and safe if FS $\geq$ 1.3 (Watts et al. 2003), its security factor decreases by roughly 38% for the slope saturated with free draining, and by roughly 58% for the slope saturated with ice dammed draining. The slope block therefore may reach the limit equilibrium with water pressure as the triggering factor. However, many other triggering factors such as earthquake and toe erosion may affect the sensitivity of the safety factor.

3 Materials and Methods

3.1 Velocities Setting

Given that, trajectory of a block (considered punctual) is A-B (A the departure point and B the stop point). During the propagation downhill, the weight performs a driving force which is independent to the path, but only depending on the difference of level between the points A and B. Maximal velocity is defined by means of statements from the kinetic energy theorem as follows:

For translational movement:

$$W_{A-B} = \int_{V_A}^{V_B} d\left(\frac{1}{2} M V^2\right) = \frac{1}{2} M V_B^2 - \frac{1}{2} M V_A^2 = Mgh \quad (1)$$

where: $W_{A\text{-}B}$ is the work of the weight force, M is the block mass, g is the gravity force, V is the translational velocity, h is the level between the points A and B.

For rotational movement:

$$W_{A-B} = \int_{\omega_A}^{\omega_B} d\left(\frac{1}{2} J_\Delta \omega^2\right) = \frac{1}{2} J_\Delta \omega_B^2 - \frac{1}{2} J_\Delta \omega_A^2 = Mgd\theta \quad (2)$$

where: J_Δ is the mass moment of inertia, ω is the rotational velocity, d is the distance between the axis Δ and the weight force vector, Θ is the browsed angle.

(1) Since $\omega_A = 0$, $W_{A-B} = \frac{1}{2} J_\Delta \omega_B^2 = Mgd\theta$

Assuming that the rotational movement is not uniform and Δ axis is not constant; the weight vector may fall parallel to Δ axis (thus $\Theta = 0$), and the moment of weight force becomes zero (thus $\omega_B = 0$). Therefore, the rotational kinetic energy can be cancelled at any time while the block continues to slide downhill. All these led us to neglect the rotational kinetic energy in the calibration of the theoretical values of maximal velocity.

(2) Since $V_A = 0$, $W_{A-B} = \frac{1}{2} M V_B^2 = Mgh$; hence:

$$V_B = \sqrt{2gh} \tag{3}$$

Figure 3 shows the numerical model of slope profiles between points A and B (extracted from SRTM release), whereas Table 1 shows theoretical maximal velocities of the fallen blocks.

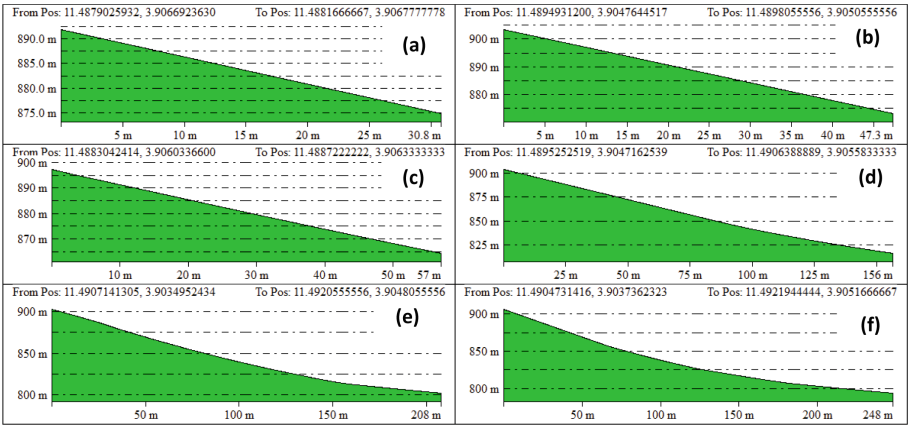

Fig. 3. Slope profiles between points A and B. (a) Block n°1, (b) block n°2, (c) block n°3, (d) block n°4, (e) block n°5, (f) block n°6

Table 1. Fallen block shapes and theoretical maximal velocities. $\varphi = 2600$ kg/m^3, g = 9.81 N/kg. The uncertainty rate is 10%

	Dimension	Volume (m^3)	Height (m)	Velocity (m/s)**
Block n°1	4 × 6 × 5	120 ± 12	30	$V_{max} = 24.26$
Block n°2	12.6 × 22 × 13.8	25 ± 3	25	$V_{max} = 22.15$
Block n°3	4 × 10 × 6	585 ± 58	40	$V_{max} = 28.01$
Block n°4	6.7 × 12 × 4.6	370 ± 37	85	$V_{max} = 40.84$
Block n°5	2 × (3.3 × 3.9 × 3)*	2 × 40 ± 8	100	$V_{max} = 44.29$
Block n°6	2 × (8 × 12 × 8.4)	2 × 810 ± 162	120	$V_{max} = 48.52$

*time 2 concerns the half buried block. **: $V_{max} = \sqrt{2gh}$

Table 2. Reports of geomorphology and fallen blocks geometries from the investigated slope

Location	N°	Coordinates	Altitude	Nature	Shape
Seeder		N03°54′11.8”; E11°29′25.9” to N03°54′22.0”; E11°29′16.1”	920 m	Cliff	Line
Final immobilized mass	1	N03°54′18.2”; E11°29′23.3”	870 m	Point	Extruded polygon
	2	N03°54′24.4”; E11°29′17.4”	875 m	Point	Extruded polygon
	3	N03°54′22.8”; E11°29′19.4”	868 m	Point	Extruded polygon
	4	N03°54′20.1”; E11°29′26.3”	820 m	Point	Extruded polygon
	5	N03°54′17.3”; E11°29′31.4”	805 m	Point	Extruded polygon
	6	N03°54′18.6”; E11°29′31.9”	795 m	Point	Extruded polygon

3.2 RocFall3 Program Setting

The RocFall3 code used for this study combines the two-dimensional map to the three-dimensional model. Its guidelines usage is covered by tutorial files which are installed with the program (see Rocscience Inc. 2022a) or found in the Rocscience Inc. (2022b) internet site. RocFall3 goes with lump mass and rigid mass methods. With lump mass method, the rocks are assumed to be point masses, whereas the rigid body method allows defining the rock shapes. We found it useful to define the rock shapes since the shape usually affect the rotational and translational velocities during the blocks propagation. We used the terrain generator image because it allows the importation of coordinated image and doesn't absolutely require the ad of new material region, thus we set the layer as “satellite”; also, the materials (bedrock outcrops, talus vegetal cover, and road asphalt) and their properties were rather well defined. The paths were checked according to the clearly appointed seeder plane and fallen blocks on the field (Table 2). These supported the way we defined input parameters, such as the number of rock (20 rocks overall), the likeliest translational velocity (30 and 50 m/s), and the relative rotational velocity (0° or 10°/s).

4 Results and Discussion

4.1 Analysis of Paths

As mentioned above, the simulation of paths as the rocks travel down was implemented with theoretical values, i.e. 30 m/s and 50 m/s translational velocities and 0°/s or 10°/s rotational velocities. The generated paths perfectly match to the targets of the fallen

Table 3. Statistical evaluation of the matching of simulations with field observations

Runout (m)	Field observations*		Histogram 1 (V = 30 m/s)		Histogram 2 (V = 50 m/s)	
	Number	Rate (%)	Number	Rate (%)	Number	Rate (%)
< 100	3	50	18	90	2	10
100 - 200	1	16.66	1	5	12	60
> 200	2	33.33	1	5	6	30

See relative runouts in Fig. 3

blocks, especially at 50 m/s translational velocity. There are long and short almost rectilinear and curved/deviated rock paths (see Figs. 4 and 5). At the first step, the long almost rectilinear paths suggest that the slope may have undergone voluminous mass movements. For example, with about 2 × (8 × 12 × 8.4) m^3, the fallen block n°6 was the most voluminous we encountered on field (whereas the other blocks fall between 4 × 6 × 5 m^3 and 6.7 × 12 × 4.6 m^3); its translational runout exceeded 350 m on a vegetal covered slope. At the second step, the curved/deviated and short/long paths suggest that the slope presents an irregular topography.

4.2 Statistical Analysis

The statistical analysis of the rock paths is summarized in Fig. 6. Let's subdivide the runouts in three classes: the short length (< 100 m), the medium length (100 – 200 m), and the long length (>200 m). Table 3 shows how perfectly the 30 m/s translational velocity histogram matches with short length runout, whereas the 50 m/s translational velocity histogram matches with long length runout.

4.3 Study Gap

In this work, the model was built in a timely manner based solely on readily available data such as slope irregular topography, rock and vegetal cover properties; the underlying surface morphology and soil properties were ignored.

5 Conclusion

This study investigated the rockfall hazard process from the Yaounde area's rocky hills using RocFall3 program through a case study, of eastern slope of the Mbankolo rocky hill. The rockfall simulation was calibrated to answer theoretical support (i. e., 30–50 m/s translational velocity and 0 or 10°/s rotational velocity). Overall, with 50 m/s translational velocity, the paths perfectly match to the targets of the fallen blocks. They are long and short almost rectilinear and curved/deviated paths. The long almost rectilinear paths suggest that the slope may have undergone voluminous mass movements. The curved/deviated and short/long paths suggest that the slope presents an irregular topography. 30 m/s translational velocity matches with short length runout, whereas 50 m/s

translational velocity matches with long length runout. However, the study considered the slope topography only with its rocks and vegetal cover properties; and ignored the underlying surface morphology and soil properties. This gap could be completed in extended research works.

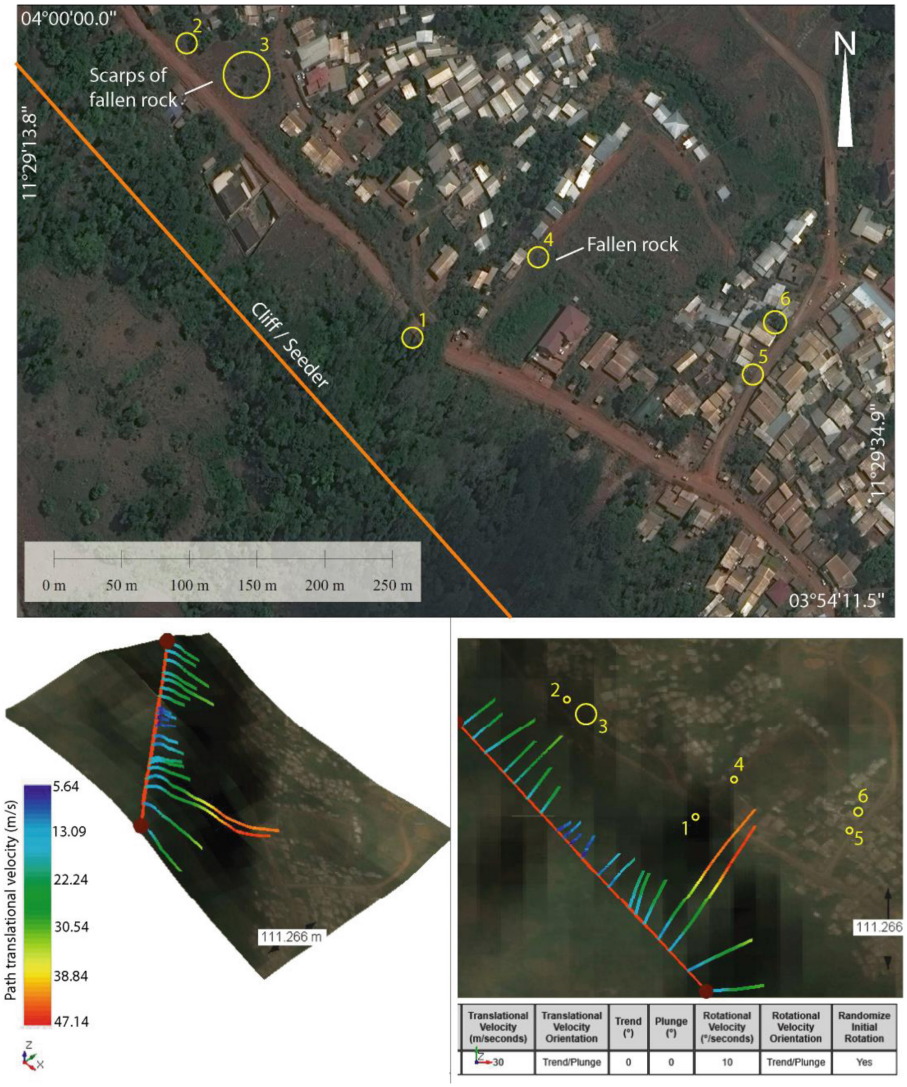

Fig. 4. Computation of rock paths with translational velocity calibrated 30 m/s. The satellite image is from Google Earth

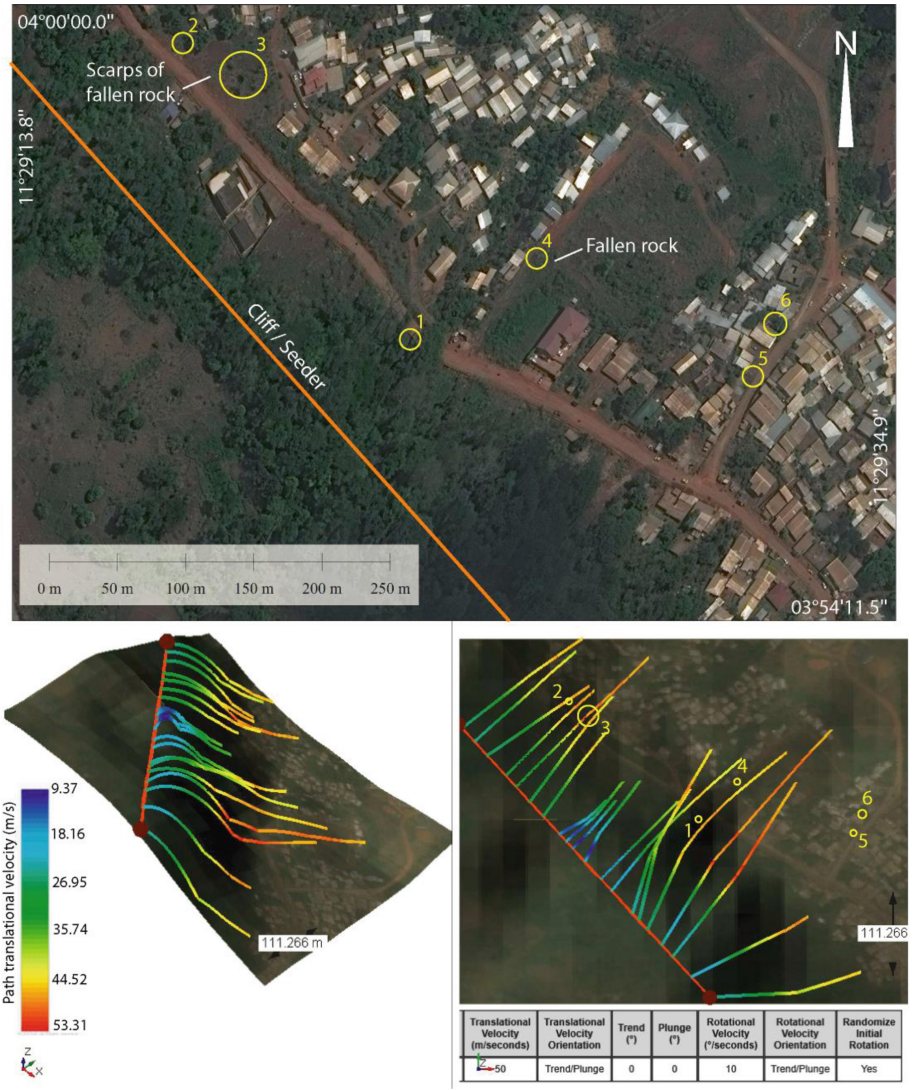

Fig. 5. Figure 4 continued, with translational velocity calibrated 50 m/s

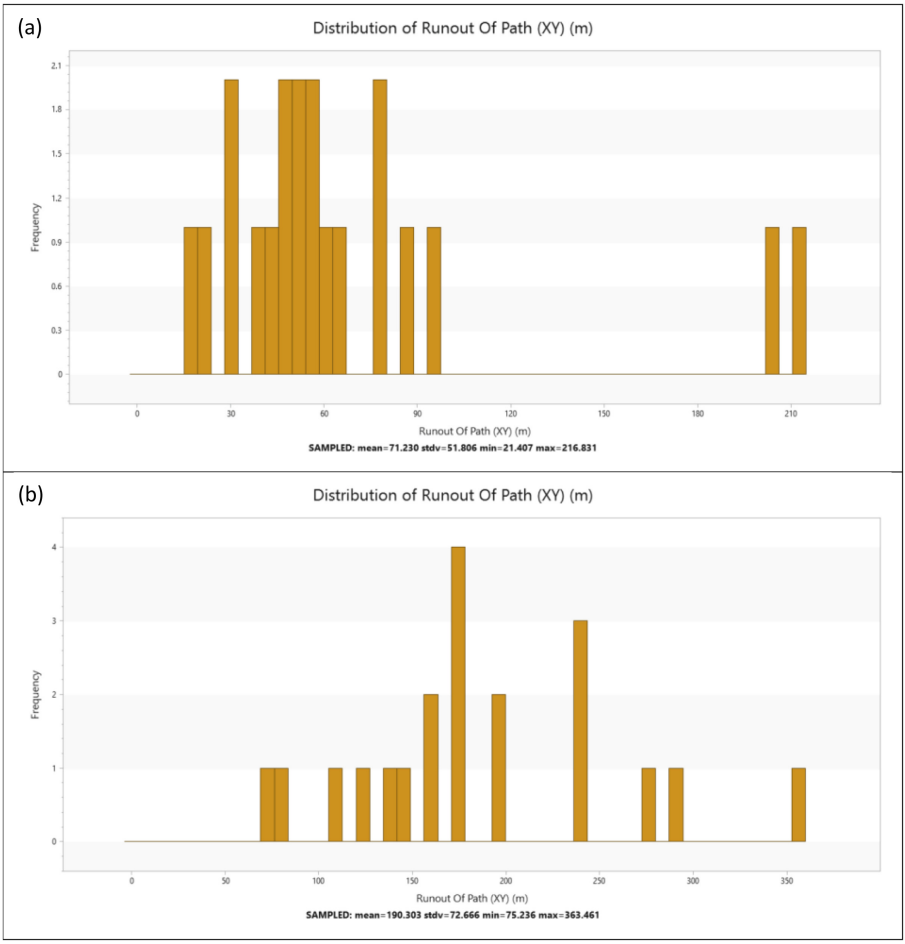

Fig. 6. Histogram of path runouts from (a) 30 m/s and (b) 50 m/s translational velocities

Acknowledgements. The authors are thankful to Rocscience Inc. Technical support team for providing a 15-day product key for RocFall3 program, as well as materials on "getting started" with this program.

References

Bissaya, R., Medjo, E.R., Ghogomu, R.T., Njom, B.: Characterization of rock mass and its influence on rock slopes stability with survey data from Yaounde (Cameroon). *Proceedings of the 2nd International Conference Advances in Rock Mechanics*, Paper number: TR 101, Tunirock 2022, Hammamet, Tunisia, March 2022 (2022a).

Bissaya, R., Medjo, E.R., Njom, B., Ghogomu, R.T.: A case study on the stability analysis and rockfall assessment on a massif at risk, Mbankolo, Camerooon. *Arab. J. Geos.*, 15:1499 (2022b).

Bissaya, R., Ngamy, K.A., Medjo, E.R., Ghogomu, R.T., Njom, B.: NR XP P94-424 standard shear tests for estimating the mechanical properties of rock joints sampled from Yaounde gneisses (Cameroon). *J. Geomech. Geoeng.*, 1, 39–50 (2023).

Hungr, O., Leroueil, S., Picarelli, L.: The Varnes classification of landslide types, an update. *Landslides*, 11, 167–194 (2014).

Lu, P., Latham, J.-P.: Developments in the assessment of in-situ block size distributions of rock masses. *Rock Mech. Rock Eng.*, 32, 29–49 (1999).

Merritt, A.H., Baecher, G.B.: Site characterization in rock engineering *22nd U.S. symp. On Rock Mechanics*, 49–66 (1981).

Palmström, A.: RMi – a rock mass characterization system for rock engineering purposes. *PhD Thesis*, University of Oslo, Norway, 409p (1995).

Palmström, A.: Measurement and characterization of rock mass jointing, In Sharma, V.M., Saxena, K.R. (Eds). In-situ characterization of rocks. Chapter 2, A. A. Balkema publishers (2022).

Rocscience Inc.: RocFall3 Basic Physics - Theory manual. Toronto, 50p (2022a).

Rocscience Inc.: https://www.rocscience.com/help/rocfall3/tutorials/ last accessed 26/12/2022 (2022b).

Ruiz-Carulla, R., Corominas, J., Mavrouli, O.: Analysis of rockfalls by means of a fractal fragmentation model. Rock Mech. Rock Eng., 1–23 (2019).

Varnes, D.: Slope movement types and processes. In Shuster, R.L., Krizek, R.J. (Eds), Landslides, Analysis and Control, Transportation Research Board, Special report N° 176, National Academy of Sciences: Washington, DC, USA, 11–33 (1978).

Watts, C.F., Gilliam, D.R., Hrovatic, M.D., Hong, H.: Rock slope stability computerized analysis package, Appendix B – An Introduction to plane failure safety factor calculations including artificial support, Radford University Office, 13 p (2003).